ICES Journal of Marine Science, 57: 1128–1142. 2000
doi:10.1006/jmsc.2000.0800, available online at http://www.idealibrary.com on IDEAL®

Inference of material properties of zooplankton from acoustic and resistivity measurements

Dezhang Chu, Peter Wiebe, and Nancy Copley

Chu, D., Wiebe, P., and Copley, N. 2000. Inference of material properties of zooplankton from acoustic and resistivity measurements. – ICES Journal of Marine Science, 57: 1128–1142.

A laboratory apparatus has been developed and used to infer the sound speed and density contrasts of live zooplankton. The sound speed contrast is determined from acoustic measurements of travel time (time-of-flight) and from the resistivity measurements of volume fraction. The density can then be inferred by applying the phase-compensated distorted wave born approximation (DWBA) model based on the attenuation measurement. For the decapod shrimp (*Palaemonetes vulgaris*), the inferred sound speed contrast found by using three different methods, namely the two-phase ray model (time average), the compressibility model (Wood's equation), and the DWBA model (scattering theory), is quite consistent, while the inferred density contrast agrees with the measured density reasonably well. The influence of ambient pressure on the sound speed and density contrasts has also been measured using a pressure vessel. The results indicate that the density contrast remains essentially unchanged under different pressure, but the sound speed contrast increases about 2.0% with pressure changing from 0 dbar to about 350 dbar. Although this 2.0% change in sound speed contrast only causes a moderate change in estimating biomass for a decapod shrimp, it could cause a much larger bias for weaker scatterers with the same amount of change in sound speed contrast (up to 20 dB). The most important advantage of this newly developed material properties measuring system is its potential applicability to the *in situ* determination of acoustic properties of zooplankton.

Key words: zooplankton, material properties, acoustic scattering, resistivity.

Received 11 October 1999; accepted 11 April 2000.

D. Chu: Department of Applied Ocean Physics and Engineering, Woods Hole Oceanographic Institution, Woods Hole, MA 02543, USA. P. Wiebe, and N. Copley: Department of Biology, Woods Hole Oceanographic Institution, Woods Hole, MA 02543, USA.

Introduction

Conventional pump and net samplers can provide information on biomass, size distribution, patchiness, and time evolution of marine animals (Miller and Judkins, 1981; Frost and McCrone, 1974; Wiebe *et al.*, 1976; Wiebe, 1988). Although such information is crucial for understanding the marine planktonic ecosystems, these sample systems provide only discrete and sparse information, and the surveys are time consuming and relatively inefficient. In contrast, acoustic remote sensing techniques provide indirect measurements, but cover a much larger survey area/volume in a relatively shorter time period. Extensive applications involving acoustic techniques in zooplankton studies have been reported by various investigators over the past 20 years (Holliday and Pieper, 1980, 1995; Holliday *et al.*, 1989; Stanton *et al.*, 1987, 1993, 1994a,b, 1998a,b; Foote *et al.*, 1990a; Chu *et al.*, 1992, 1993; Greene *et al.*, 1988, 1991, 1994; Wiebe and Greene, 1994; Wiebe *et al.*, 1990, 1996, 1997; GLOBEC, 1991, 1993).

Since acoustic methods are indirect measurements, scattering models are required to convert the directly measured acoustic quantities, such as volume scattering strength or target strength, to biological quantities such as abundance and biomass. Accurate conversion models are difficult to develop because of the complexities of the geometrical, physical, and environmental uncertainties associated with the scattering objects.

Acoustic scattering models for zooplankton have evolved from the simplest geometry involving spheres and infintely long cylinders (Anderson, 1950; Faran, 1951) to prolate spheroids (Yeh, 1967), finite straight cylinders (Stanton, 1988), finite deformed objects

1054–3139/00/041128+15 $30.00/0

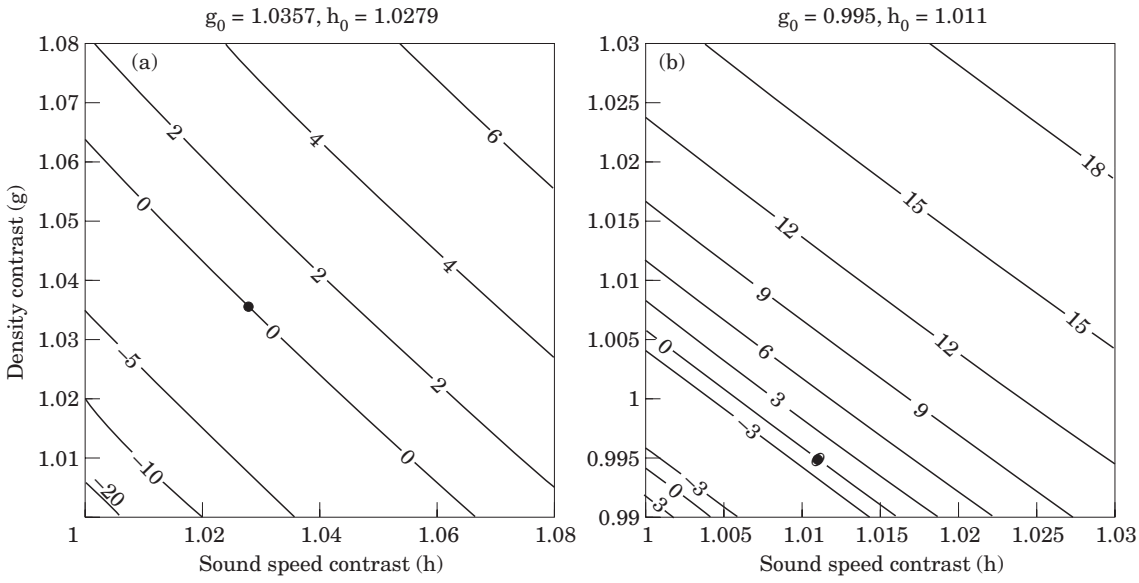

Figure 1. Isolines of the bias in target strength estimate (dB) as a function of density and sound speed contrasts, g and h based on the distorted wave Born approximation (DWBA). Two pairs of g_0 and h_0 are the actual density and sound contrasts of the zooplankton, any other combinations of g and h will result in bias in target strength estimate except those on the zero contour line.

(Stanton, 1989; Ye *et al*., 1997), and most recently to arbitrarily shaped weakly scattering objects (Stanton *et al*., 1998b). All of these models have focused on the geometric aspect of the scattering model and have assumed the known material properties, i.e. sound speed and density contrasts (h and g). In many cases, values of g and h are adjusted within reasonable limits to fit the directly measured acoustic data. Wiebe *et al*. (1997) showed a diversity of results when choosing different modelling parameters g and h used by various investigators, where g varied from 1.007 to 1.12 and h varied from 1.0279 to 1.09. Contrary to the extensive studies of scattering models, material properties of zooplankton, g and h, have not been well investigated. There are only limited data of material properties of zooplankton reported in literature (Greenlaw, 1977; Kogeler *et al*., 1987; Foote, 1990b; Foote *et al*., 1996), and all of these published data are exclusively based on the *ex situ* measurements mainly due to the difficulties of conducting the conventional measurements *in situ*. The reported material properties vary from 0.9862 to 1.0622 for g, and from 0.9978 to 1.0353 for h (some shelled animals such as pteropods can have much larger g and h). However, to fit the acoustic data, g and h beyond these ranges have also been used (Holliday and Pieper, 1980; Wiebe *et al*., 1997). Given the complex compositions of animals and very different environmental conditions and because of the unavailability of the direct measurements of g and h were not available, those choices of g and h are not unreasonable and have been used to interpret the acoustic data. However, in particular model/data comparisons, the values used in the model may not necessarily reflect the actual values appropriate to the data, and could cause substantial errors in estimating zooplankton biomass and spatial distribution.

A more systematic analysis can illustrate how significant the impacts are on the estimated target strength if g and h vary within a reasonable range. For weak scatterers (an appropriate assumption for the majority of zooplankton species), it can be shown that the differential backscattering cross section is proportional to the square of the sum of the deviations of sound speed and density contrasts from unity (Chu and Ye, 1999):

$$\sigma_{bs} \alpha (\Delta h + \Delta g)^2, \tag{1}$$

where, $\Delta h = h - 1$ and $\Delta g = g - 1$. Assuming the true g and h values for an animal are g_0 and h_0, respectively, changing g and/or h by a small amount in either direction can have a profound impact on the estimated target strength (Fig. 1). A significant influence of the material properties on the target strength is illustrated using two different g_0 and h_0 pairs considered as being representative for euphausids and copepods (Fig. 1a and b), respectively. It is clear that for both types of animals, a few percentage change in g and h would result in as much as 20 dB error in estimating target strength, corresponding to a 100-fold uncertainty in abundance and/or biomass estimates.

Obviously, due to the uncertainties in g and h, potential errors in estimating the abundance and/or biomass are currently unavoidable. The methods of

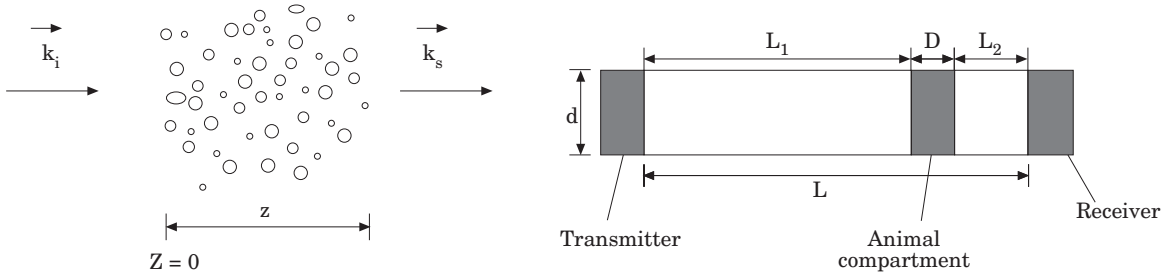

Figure 2. Scattering by a cloud of randomly distributed fluid scatterers due to a plane incident wave, a quasi-1D problem. $\vec{k}_i$ and $\vec{k}_i$ are incident and scattered wave vectors, respectively. (a) An infinite domain; (b) a finite domain with a slab of inhomogeneities (animals). The distance between the transmitter and receiver is L, the thickness (width) of the slab is D. The intensity at the receiver is I_o when animals are absent and I_s when animals are present in the slab.

measuring the physical properties of density of and sound speed in zooplankton *in situ* are extremely demanding, and new techniques are required.

Methods

Sound speed contrast

Due to the complex shapes and small sizes of zooplankton, it is not practical to measure the sound speed contrast of zooplankton directly. The method used by various investigators is to measure the sound speed or sound speed contrast in a mixture of zooplankton and seawater (Greenlaw, 1977; Kogeler *et al.*, 1987; Foote, 1990b; Foote *et al.*, 1996). To illustrate this, let us consider a simple quasi-1D problem. A plane incident wave e^{ikz}, where k is the wavenumber and z is the range, propagates through a slab composed of a cloud of scatterers (Fig. 2a). At position z, the arrival time, or the time of flight, with and without the presence of the scatterers are different because of the different acoustic properties of the seawater and the scatterers. For weak scatterers such as zooplankton, the sound speed contrast h is close to unity and can be written as:

$$h = \frac{c_z}{c} = 1 + \frac{\Delta c_z}{c} = 1 + \Delta h, \tag{2}$$

where c_z and c are sound speeds in zooplankton and seawater, respectively. $\Delta h = h - 1 \ll 1$ and $\Delta c_z = c_z - c$. To infer the sound speed contrast from the measurable arrival time and the corresponding volume fraction, ϕ (the ratio of the volume of the inhomogeneities to the total volume of the mixture), three theoretical models are used here: (i) two-phase ray model; (ii) compressibility model; and (iii) distorted wave Born approximation (DWBA) model.

Two-phase ray model (time average)

For an acoustic wavelength much shorter than the characteristic dimension of the inhomogeneities, the time average model (Wyllie *et al.*, 1958; Telford, 1984) can be used to infer the sound speed in the inhomogeneities. The method is based on the ray concept and is more applicable to a two-phase mixture. The sound speed and the volume fraction are linked by:

$$\frac{1}{c_m} = \frac{\phi}{c_z} + \frac{1-\phi}{c}, \tag{3}$$

where c_m and c_z is the sound speed in the mixture, respectively. The volume fraction, ϕ, is defined as the ratio of the volume of the zooplankton (V_z) to that of the total seawater-zooplankton mixture ($V_m = V_w + V_z$, where V_w is the volume of water),

$$\phi = \frac{V_z}{V_m}. \tag{4}$$

Defining a sound speed contrast of the mixture as $h_m = c_m/c$, Equation (3) can be rearranged as:

$$\frac{1}{h_m} = \frac{\phi}{h} + 1 - \phi. \tag{5}$$

Since $h_m = 1 + \Delta h_m$ with $\Delta h_m \ll 1$, solving the above equation for h by ignoring the second order of Δh_m leads to:

$$h_{TA} = \frac{1}{1 - \Delta h_m/\phi}, \tag{6}$$

where the subscript TA stands for time average.

For a geometry in which the total distance between the transmitter and receiver is L and the thickness of the animal layer is D (Fig. 2b), the travel time when animals are present is $t_m = D/c_m + (L - D)/c$. The sound speed difference can be expressed in terms of the measurable travel time difference as:

$$\Delta h_m^{-1} = \frac{\Delta c_m}{c} \approx -\frac{\Delta t_m}{t_D}, \tag{7}$$

where $\Delta c_m = c_m - c$ and $t_D = D/c$ is the travel time required for an acoustic wave travelling over a distance of D (the thickness of the animal layer) without the presence of animals. Substituting Equation (7) into quation (6) leads to:

$$h_{TA} \approx \frac{1}{1 + \Delta t_m/(t_D \phi)}. \tag{8}$$

For negative Δt_m, representing a faster sound speed in zooplankton, the denominator is less than unity and h_{TA} is greater than unity. For positive Δt_m, the sound speed contrast h_{TA} will be less than unity.

Compressibility model (Wood's equation)

The Wood's equation is based on the assumption of additivity of compressibility (Urick, 1947):

$$\frac{1}{\rho_m c_m^2} = \frac{\phi}{\rho_z c_z^2} + \frac{1-\phi}{\rho c^2}, \tag{9}$$

where ρ_m, ρ_z and ρ are densities of the mixture, zooplankton, and water, respectively. Solving Equation (9) for h $\left(\frac{c_8}{c}\right)$, we obtain:

$$h_{WE} = h_m \sqrt{\frac{g_m \phi}{g[(\phi - 1) g_m h_m^2 + 1]}}, \tag{10}$$

with

$$g_m = \phi g + (1 - \phi), \tag{11}$$

where subscript WE stands for Wood's equation and $g_m = \rho_m/\rho$ and $g = \rho_z/\rho$ are the density contrasts of the mixture and the zooplankton, respectively. Note that Equation (10) depends not only on the sound speed contrast, but also on the density contrast of the zooplankton.

DWBA model (scattering theory)

The scattering theory is based on the dispersion relation derived from a quasi-1D problem of a plane wave propagating through a cloud of scatterers (Fig. 2a) given by Lax (1951):

$$k_m^2 = k^2 + 4\pi n f_{scat}(\vec{k}_i, \vec{k}_i), \tag{12}$$

where k_m and k are wave numbers in the mixture and water, respectively, $f_{scat}(\vec{k}_i, \vec{k}_i)$, the scattering amplitude in the forward direction, and n, the number of animals (scatterers) per unit volume. For weak scatterers, $4\pi\eta f_{scat}(\vec{k}_i, \vec{k}_i) \ll k^2$, Equation (12) reduces to (Ishimaru, 1978):

$$k_m = k + \frac{2\pi n f_{scat}(\vec{k}_i, \vec{k}_i)}{k}. \tag{13}$$

The DWBA expression of the scattering amplitude in the forward direction $f_{scat}(\vec{k}_i, \vec{k}_i)$ is found to be (Chu and Ye, 1999):

$$f_{scat}(\vec{k}_i, \vec{k}_i) = -\frac{k^2}{2\pi} V \Delta h, \tag{14}$$

where V is the volume of the individual scatterer. Substituting the above equation into Equation (13), we have:

$$k_m = k - nVk\Delta h = k - k\phi\Delta h, \tag{15}$$

where ϕ is the volume fraction of the animal. By defining $\Delta k_m = k_m - k$ and $\Delta c_m = c_m - c$, we find:

$$\frac{\Delta k_m}{k} \approx -\frac{\Delta c_m}{c}. \tag{16}$$

Combining Equations (15), (16) and using (7), we obtain the relation between the desired sound speed contrast h and the measured Δt_m and ϕ:

$$h_{DWBA} = 1 + \Delta h = 1 - \frac{\Delta t_m}{t_D \phi} = 1 + \frac{\Delta h_m}{\phi}. \tag{17}$$

Obviously, if the sound speed in zooplankton is faster than that in the water, the travel time difference involving the mixture Δt_m will be negative and the sound speed contrast h will be greater than unity. In contrast, h will be less than unity if the sound speed in zooplankton is slower than that in the water.

Volume fraction

In order to use these models to determine the sound speed contrast of zooplankton, the volume fraction must first be determined. The challenge in measuring the volume of zooplankton arises from the difficulty in separating zooplankton from the water attached to their bodies. The measurement of displacement volume has been used by various investigators as a convenient method to determine zooplankton volume (Wiebe, 1975). For small organisms such as copepods, interstitial water content (i.e. water trapped between the bodies of the animals) may cause significant errors when measuring the displacement volume. A method of computing the zooplankton volume based on 2D videotaped and digitized images was proposed by Foote *et al.* (1996). To compute the volume from a 2D image, they assumed the symmetry about the longitudinal axis of the animal. It is quite possible that such an approach will inevitably introduce some error which could easily exceed a few percentage or more. Most importantly, both methods involve direct measurements and are almost impossible to be used for *in situ* measurement of animal volume.

One of the indirect methods that can be used to determine the volume fraction is the resistivity (conductivity) method, which is widely used in geophysical applications to estimate the porosity of the sediment (Winsauer, 1952; Evans, 1992). Owing to the fact that the resistivity of sediment and water are different, different volume fractions of water–animal mixture should result in different resistivity readings. In practice, instead of determining the absolute resistivity, a relative and measurable quantity, the formation factor, F, is used to describe the relation between the volume fractions and the *relative* resistance readings:

$$F(\phi_p)=\frac{R_m(\phi_p)}{R_w}, \tag{18}$$

where ϕ_p is the porosity, R_m and R_w are resistances of water–animal mixture and water only, respectively. Strictly speaking, the formation factor is a function of volume fraction, geometric shape, and orientation of the particles of sediment grains, and the ratio of the resistivity of water to that of sediment. However, for saturated or unsaturated sediments with a low or moderate porosity, the sediment can be approximately described as homogeneous and isotropic media. In addition, since the sediment is considered non-conductive, the formation factor can be approximately modelled as independent of the shape and orientation of the sediment particles, as well as the resistivity ratio. Extensive research has been carried out to model the formation factor in terms of the porosity of the sediments, i.e. the volume fraction of water (Archie, 1942; Winsauer *et al*., 1952; Jackson, 1978; Schopper, 1967; Mualem, 1991; Evans, 1992). The models are either empirical or theoretical.

All these models have been used to determine the porosity of the saturated and unsaturated sediments by measuring the formation factor given in Equation (18). In our current application, it is more convenient to work with volume fraction rather than porosity. The reciprocal relation between the porosity (ϕ_p) and the volume fraction (ϕ) is simply:

$$\phi_p=1-\phi. \tag{19}$$

Since the shapes of zooplankton are very complicated and the resistivity of the zooplankton is essentially unknown, finding the exact relations between the formation factor and the geometric and physical properties of the zooplankton is extremely difficult. A simple and convenient way is to use an empirical approach. One of the empirical models widely used is the power law proposed by Archie (1942) and extended by Winsauer *et al*. (1952):

$$F(\phi)=a\phi_p^{-m}=a(1-\phi)^{-m}, \tag{20}$$

where constants a and m can be determined empirically.

Density contrast

The density of zooplankton can be measured directly or indirectly. Direct measurements involve placing the animals either in a density–gradient fluid (Linderstrom-Lang, 1937; Linderstrom-Lang *et al*., 1938; Kogeler *et al*., 1987) or in a series of density bottles (Greenlaw, 1977). The indirect measurements primarily involves two approaches. One is by measuring the weight and volume of water displaced by the animals, and then computing the density of the objects (Lowndes, 1942; Wiebe *et al*., 1975). The other is based on measuring the sinking rate of the objects (Gross and Raymont, 1942; Salzen, 1956).

However, all of the above approaches have to be done in the laboratory and require handling of the animals. To infer the density contrast *in situ*, we use an indirect approach by measuring the change (reduction) of the acoustic intensity due to animals in the acoustic path. The intensity reduction results from the scattering-induced attenuation which is a function of the density contrast g, sound speed contrast h and volume fraction, ϕ, as well as geometric parameters of the animals. Since the sound speed contrast and the volume fraction of the animals can be obtained using the methods described previously II.1 and II.2, it is possible to infer g from intensity measurements in the forward direction. The method of using measuring the forward scattering intensity to extract information about scatterers has been previously used by many investigators on different types of scatterers. Foote *et al*. (1992), and Furusawa *et al*. (1992) studied the extinction cross section of fish empirically, while Ye (1996) provided a detailed description of the forward scattering due to the fish swimbladder, a pressure release boundary condition. Sheng and Hay (1988) and Thorne *et al*. (1991) studied the scattering by suspended sediments by using a rigid movable sphere model in predicting the sound attenuation (extinction) due to the suspended sand particles. For the current problem involving zooplankton, a weakly scattering scenario and a fluid boundary condition will be considered. Let I_s and I_o denote the intensities at the receiver (Fig. 2b) with and without the presence of animals, respectively, the ratio of the two intensities, a measurable quantity, can be expressed as:

$$r_I=\frac{I_s}{I_o}=e^{-\sigma_\Sigma^z}, \tag{21}$$

with

$$\sigma_\Sigma=n_0\int i\rho_n(p)\sigma_e(p)dp, \tag{22}$$

where ρ_n is the probability density function (PDF) of number density, with n_0 being the total number of animals in a unit volume and $\int n_0^{\infty}{}_{-\infty}\rho_n(p)dp=1$. The parameter p refers to the properties of the aggregated scatterers, σ_e is the extinction cross section of the

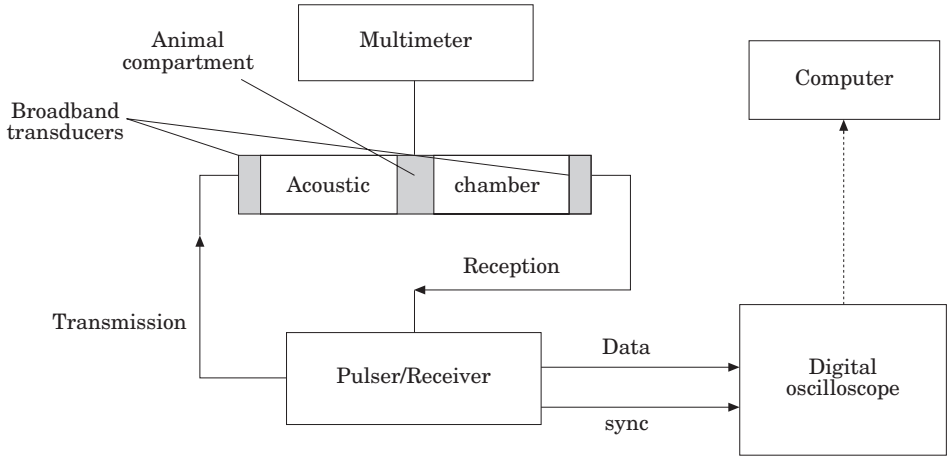

Figure 3. Schematic diagram of the measuring system.

individual organism which, by the forward scattering theorem or optical theorem, can be expressed as (Ishimaru, 1978):

$$\sigma_e(p) = \mathrm{Im}\left\{\frac{4\pi}{k} f_{scat}(\vec{k}_i, \vec{k}_i)\right\}, \tag{23}$$

where $f_{scat}(\vec{k}_i, \vec{k}_i)$ is the scattering amplitude in the forward direction and parameter p is implicitly included in the scattering function $f_{scat}(\vec{k}_i, \vec{k}_i)$. For an arbitrarily-shaped weakly scattering marine organism, a simple way of computing the scattering amplitude is to use the DWBA (Chu *et al*., 1993; Stanton *et al*., 1998b). However, it has been shown that due to the inherent deficiency of the DWBA, a direct application of the DWBA to the current problem will fail since it predicts a zero imaginary part of the scattering in the forward direction and causes a vanishing extinction cross section. To overcome this shortcoming of the DWBA, a heuristic phase-compensated DWBA model has been developed to include the scattering-induced attenuation by introducing a phasor term (Chu and Ye, 1999) and can be expressed in a general form:

$$f_{scat}^{PC-DWBA}(\theta_s) = f_{scat}^{DWBA}(\theta_s) e^{i\Phi(\theta_s)}, \tag{24}$$

where $f_{scat}^{DWBA}(\theta_s)$ is the scattering amplitude obtained using DWBA, and $\Phi(\theta_s)$ is the phase compensation (Equation (22) Chu and Ye, 1999 for a prolate spheroid).

Using Equations (21)–(24), a least-square (LSQ) criterion can be used to obtain the optimized density contrast g and the characteristic size s (for spherical objects, s could be the mean radius) of the animals. Since the system is broad band, the LSQ can be performed over the bandwidth (BW) of the received signal:

$$Q(g,s) = \int_{BW} [r_I(f; g,s) - \hat{r}_I]^2 df, \tag{25}$$

where r_I and $\hat{r}_I$ are theoretical predictions and measured data, respectively. s and g are the characteristic size and the density contrast of zooplankton, respectively. The integral is performed over the usable frequency band (f). Minimizing Q(g,s) with respect to the density contrast g and size parameter s, we can obtain the estimated $\hat{g}$ and $\hat{s}$ based on the best fit.

In actual computations, it is much easier to work with a mean extinction cross section

$$\langle \sigma_e(p) \rangle = \int \rho_n(p) \sigma_e(p) dp. \tag{26}$$

This way, we only need to invert the mean size of the animals instead of the size distribution of the animals. In other words, we use a uniform PDF to approximate the actual size distribution.

Experiment

Experiment setup

In order to measure the material properties of zooplankton using the equations described above, an experimental system has been developed. The system consists of the mechanical apparatus, an acoustic pulse-echo system, and a resistivity measuring device (Fig. 3).

The mechanical apparatus includes two major parts: an acoustic chamber and a pressure vessel which allows the experiments to be conducted under pressure (Fig. 4). The core component of the mechanical apparatus is the acoustic chamber. The animals are confined in the animal compartment by two thin rubber sheets (natural latex sheeting with a thickness of 0.04 mm) in the direction perpendicular to the axis of the chamber. The

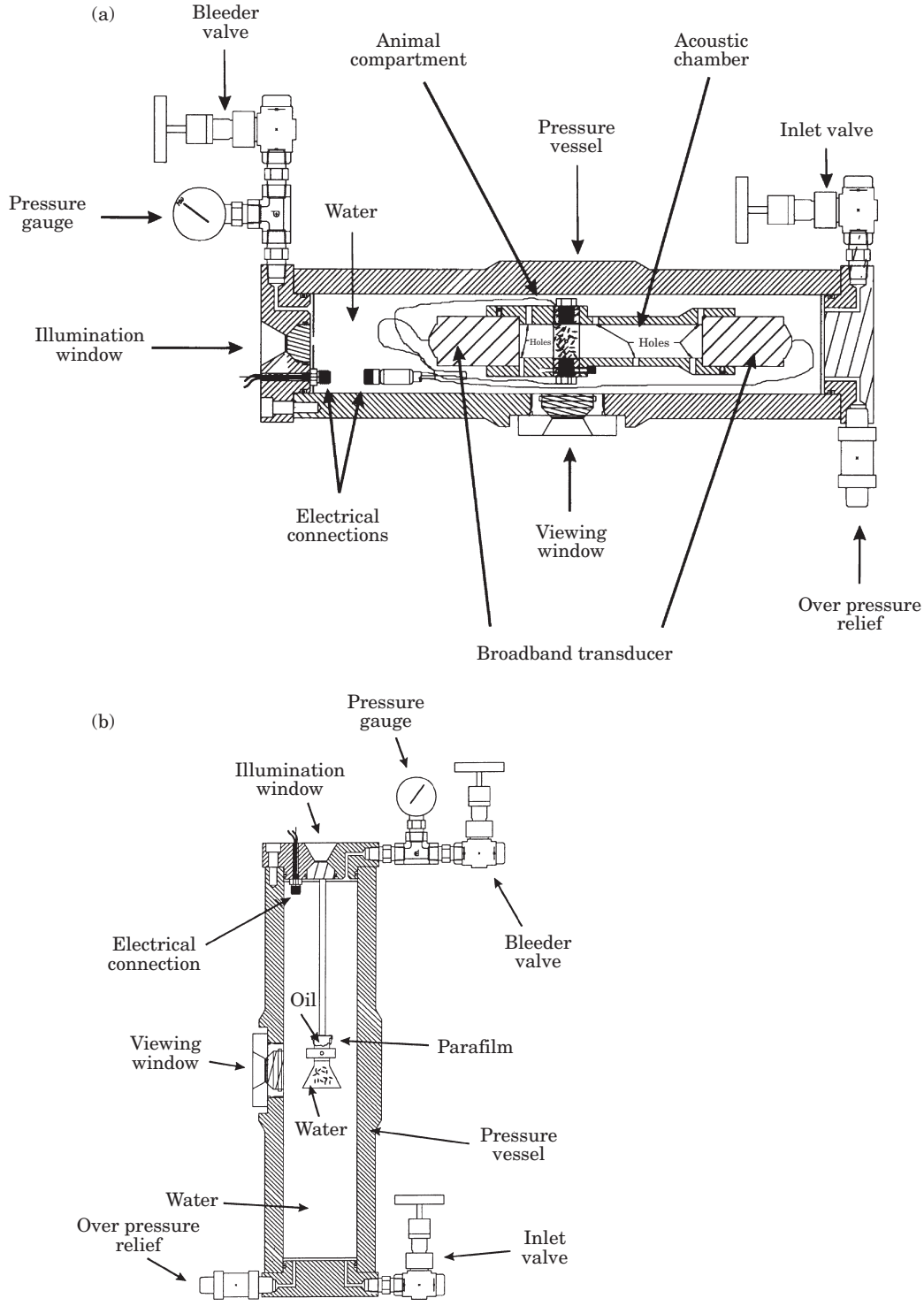

Figure 4. Drawing of the acoustic chamber and the pressure vessel which were used in the experiments to determine the sound speed and density contrasts. (a) Acoustic chamber in the pressure vessel. The dimensions of the chamber illustrated in Figure 2 are $L=16.3$ cm, $D=2.0$ cm, $L_1=10.7$ cm, $L_2=3.6$ cm, and $d=2.54$ cm (1 inch). (b) Density measurement device (flask and the holding device) in the pressure vessel.

width of the compartment in the direction of the acoustic path (parallel to the axis of the acoustic chamber) is 2 cm. The distance between one sheet to the transmitter (left) is 9.7 cm, while the distance between the other sheet and the receiver (right) is 2.6 cm (Fig. 4a). Two electrodes used for resistivity measurements are mounted on the front and back sides (not shown in Fig. 4a, since they would block the view of the animals) of the animal compartment, facing each other. There are two threaded holes, on the top and bottom of the animal compartment facing each other, which allow animals to be inserted and released. These two holes are sealed with two plastic pipe screws to retain the animals after they are inserted into the compartment. Two broadband transducers (350–650 kHz, Materials Systems, Inc.) are mounted on the ends of the acoustic chamber. All wires are water proofed and external connections are made through a connector mounted on the pressure vessel. Holes in the walls of the acoustic chamber are used to release any bubbles that might be generated during the placement of the chamber in the experimental tank and the pressure vessel.

The density variation due to pressure change has to be measured separately, since the current apparatus cannot simultaneously measure the sound speed and density contrasts under pressure. To measure the density at different pressure, a flask mounted on a holding device can be placed at the same height of the viewing window (Fig. 4b). A light source is provided through the illumination window to allow the observer to see the fluid level in the flask and read the marks on the flask. To measure the density change under pressure, the mixture of animal and water is first poured into the flask and then food oil is added into the flask, forming a distinctly visible interface between oil and the seawater until the flask is full. The flask is then covered with a membrane (para film) to seal the flask, but still allow the pressure to be exerted on the mixture. After filling the pressure vessel with water and putting the cap on, the interface level can be observed through the viewing window and recorded before and after pressure is applied.

The Pulser/Receiver system (Panametrics, Inc., Model 5800PR) is capable of transmitting and receiving acoustic signals either in a bistatic (transmission) or a monostatic (backscattering) configuration. It transmits an impulse with a bandwidth of 35 MHz. The analog output from the Pulser/Receiver is then digitized with a digital scope (LeCroy Corp., Model 9310C), coherently averaged and then stored on a floppy disk for later data processing. Resistivity readings can be simply obtained from a digital multimeter.

Measurements

A total of 23 live decapods (*Palaemonetes vulgaris*), with a mean length of 24 mm and mean width of 4.5 mm, were used in the experiment conducted on 22 January 1999. The acoustic properties of the animals resemble those of fluids (Chu *et al*., 1992; Stanton *et al*., 1993, 1998b). The acoustic chamber was placed in a 25 gallon tank (aquarium) where the acoustical measurements were performed. Since the resistivity and sound speed in water are sensitive to temperature, the experiment was performed in a cold room where the temperature was set at 4°C (there was 0.5°C variation in temperature due to people entering and leaving the room during the experiment). The filtered sea water was kept in the cold room for more than 12 h and its temperature was 5.2°C. Although it had not yet equilibrated with the room temperature, the temperature variation in the tank was within 0.3°C during our experiment.

It was very important to make sure that bubbles were not present during the entire experiment. To ensure this, the acoustic chamber was put in the tank overnight so that its temperature became the same as the surrounding water to prevent bubbles from being generated. To ensure that bubbles were not present, the transducers were pulled and pushed back and forth in the chamber several times to force the air bubbles out of the holes after the equilibration period. A squirt bottle filled fully with water (no air) was used to expel the bubbles by injecting water into the animal compartment.

The 23 live shrimp were divided into five groups. For each group, the animals were dried carefully by using paper towels and cold (natural) blowing air generated from a heat gun. The weight of the animals was quickly measured on a micro-balance to ± 0.1 mg. Then they were placed into a volumetric cylinder and their displacement volume was measured to ± 0.1 ml. The mean density of each group was then calculated by using measured weight and the displacement volume. The total mean density was obtained using the total measured weight and volume (sums of all five groups). After the volume and density measurement, the animals were kept alive in separate containers in an aquarium for at least 20 min to allow the temperature of the animals to become the same as that of the surrounding sea water. During the experiment, the animals were inserted into the animal chamber one group at a time to allow acoustic and resistivity measurements at several different volume fractions.

For each volume fraction, the acoustic and resistivity measurements were made. For the acoustic measurements, an impulse 35 MHz bandwidth was transmitted and the received signal (bistatic mode) were coherently averaged over 1000 pings and then the multimeter reading for the resistivity measurement was recorded. The readings were quite stable with less than 1% variation.

To study the variation of sound speed due to pressure change, the acoustic and resistivity measurements were made when the acoustic chamber was placed in the

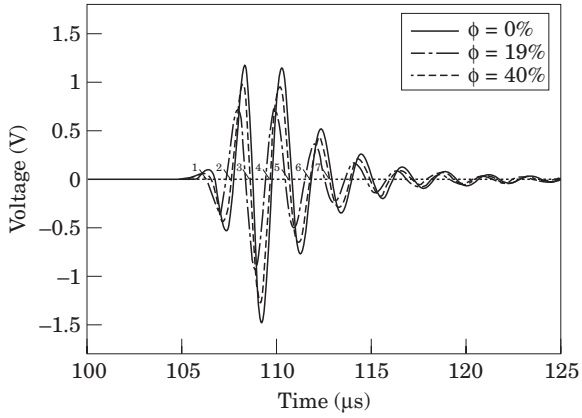

Figure 5. Waveforms of the acoustic signals in the forward direction with different volume fractions of decapod shrimp (*Palaemonetes vulgaris*). Three out of six waveforms, corresponding to six different volume fractions (0, 10%, 19%, 29%, 40% and 48%) are plotted in the figure. The transmit signal is an impulse with a bandwidth of 35 MHz while the 6 dB bandwidth of the transducers is about 300 kHz (350–650 kHz).

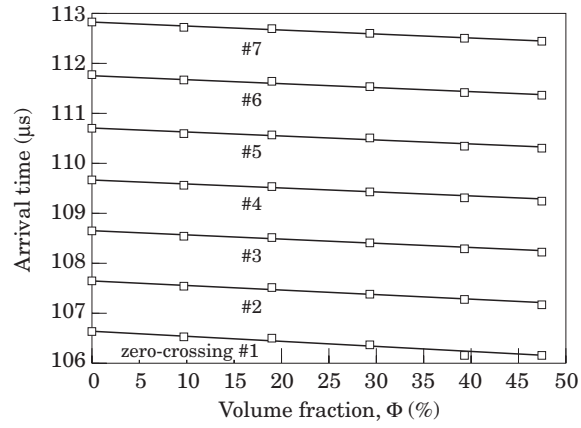

Figure 6. Linear regressions of arrival time (time of flight for acoustic wave travelling from the transmitter to the receiver) versus volume fraction, ϕ, for different zero-crossings. The number labels correspond to those in Figure 5.

pressure vessel. After all animals were placed in the animal compartment, the acoustic chamber, which was kept submerged in the water to avoid the formation of air bubbles, had a plastic bag slipped around it and filled with water. Then, the bagged chamber was carefully inserted into the pressure vessel. Waveforms and resistivity readings were recorded before and after applying a pressure up to about 350 dbar (500 psi). All 23 animals were alive after the completion of the acoustic and resistivity measurements under pressure.

To measure the density variation due to pressure change, we put 10 ml of the animal and water mixture, with an animal volume fraction of 38.5%, into the flask and recorded the levels of the water–oil interface before and after pressure was added to about 350 dbar (same as for the acoustic and resistivity measurements).

Results and discussion

The volume fraction had a significant effect on the arrival time of the transmitted signal. For the volume fractions 0, 19% and 40%, the corresponding waveforms had different arrival times, i.e., a shift of waveform horizontally (Fig. 5). The larger the volume fraction, the earlier the wave arrived, indicating a faster medium ($c_m > c$, where c and c_m are the sound speed in the pure seawater and in the animal/seawater mixture, respectively). Furthermore, there was a strong decrease in the amplitude of the signal with increasing volume fraction, resulting from the scattering induced attenuation. The waveform, however, was essentially unchanged implying that the dispersion was insignificant (Fig. 5). The signal-to-noise ratio (SNR) was very large, indicating a very high level of data quality.

Since the real arrival time is very hard to determine due to the finite bandwidth of the transducers, a relative arrival time was obtained by finding the zero crossing of the curve since dy(t)/dt is maximum at zero crossings where y(t) is the received time series. Seven zero crossings were chosen for each waveform corresponding to a certain volume fraction. Thee reference arrival times were plotted against the volume fractions and were characterized by seven straight lines which result from linear regressions on the corresponding data (Fig. 6). The linear regression curves describe the relation between reference arrival time and volume fractions very well. The slopes for all seven lines are quite consistent, with a standard deviation of 8.7×10^{-4}.

The sound speed contrasts as a function of volume fraction were computed using the three models described in Equations (6), (10) and (17) (Fig. 7). To compute the sound speed contrast with Equation (10), we used the obtained density contrast $g = 1.043$. The density was measured by measuring the displacement volume and weight (Wiebe *et al.*, 1975). It is not surprising that h computed from the DWBA model agrees with that computed from the two-phase ray model (TPRM), since by expanding Equation (6) for a small Δt_m, we obtain the same result as in Equation (17). Since the assumption of additivity of compressibility is valid only for low frequency applications, i.e. the wavelength is larger relative to the characteristic dimension of the scatterer (Ye and McClatchie, 1998), the volume fraction dependence of sound speed contrast indicated possible errors in using the compressibility model (CM) for the current application. For the animals used in the experiment, the equivalent spherical radius of the organisms was $a_{eq} = 3.54$ mm and at a frequency of 500 kHz, the wave length is 3 mm, which is comparable to the a_{eq}. This may invalidate the assumptions upon which the Wood's

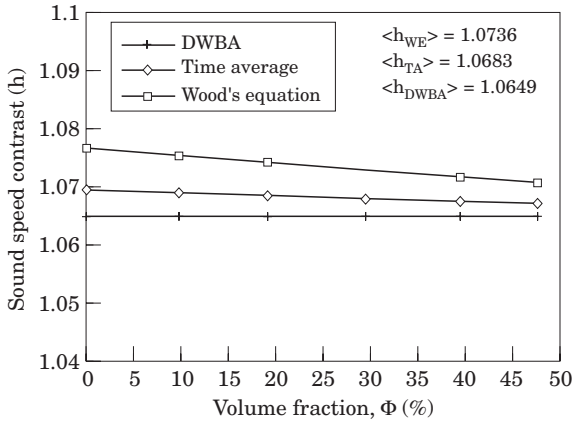

Figure 7. Sound speed contrast estimates using three different models: TPRM (two phase ray model), (6), CM (compressibility model), (10), and DWBA (distorted wave born approximation), (17). The mean values over volume fraction for each model are given on the Figure.

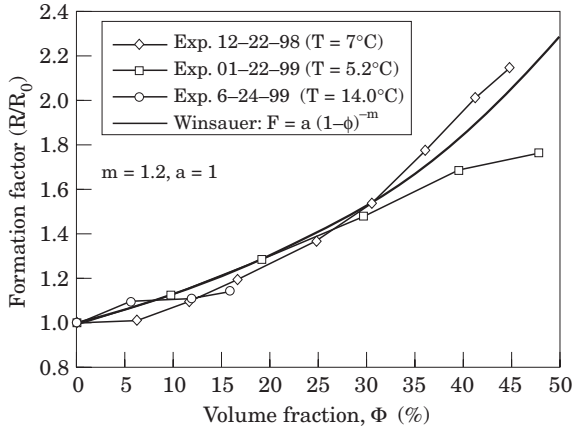

Figure 8. Formation factor $R(\phi)/R_0$ from resistivity measurements, where R_0 is the measured resistance without the animals in the animal compartment, and $R(\phi)$ is the measured resistance at the volume fraction of ϕ. There are three data sets corresponding to three experiments conducted at different temperatures. Superimposed is the heuristic model from Winauer with amplitude coefficient of a=1 and the exponential (Archie *et al.* 1952) m=1.2.

equation is based. Despite the potential errors in determining the sound speed contrast by the compressibility model, the variation in inferred h was relatively small and the agreement among the three methods was still reasonably good when compared to the mean values given in the legend of Figure 7.

The volume fractions used in Figures 5–7 were obtained from the direct measurements of displacement volume. However, to infer sound speed contrast *in situ*, the volume fraction from direct measurement would not be available. To explore the feasibility of determining the volume fraction of the animals in the compartment indirectly, the resistivity method discussed above was used in our experiment. Three independent measurements (different animals but the same species) of the formation factor versus volume fraction were made at three different temperatures (Fig. 8). The formation factor at 5.2°C corresponded to the experimental data presented in Figures 5–7. The thick solid curve was computed based on the Winsauer's formula, where the strength parameter a and power m were 1 and 1.2, respectively. Since a=1, Winsauer's formula reduced to Archie's formula (Archie, 1942). The theoretical curve based on the Winsauer's model fitted all three data sets reasonably well for $\phi<35\%$ (Fig. 8). Although the resistivity is very sensitive to the temperature, by using a normalized quantity, F, the temperature dependence has been greatly reduced, if not been removed.

Using the approximate theoretical formation factor to infer volume fraction will inevitably introduce errors. To investigate how these errors affect the sound speed estimates, we repeated the procedures in obtaining Figures 6 and 7 with the actual volume fraction ϕ replaced by the inferred $\hat{\phi}$ from the theoretical resistivity formation factor given in Figure 8.

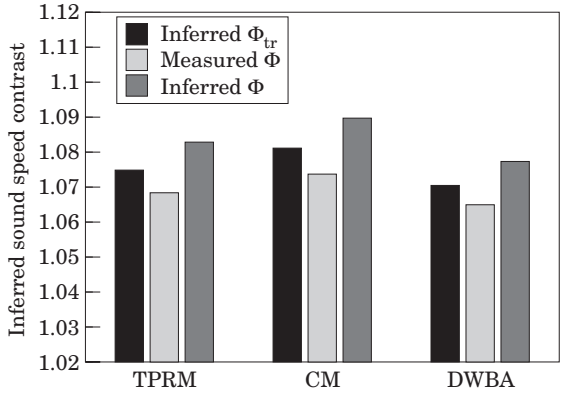

Figure 9. Inferred sound speed contrast, h, using different models: TPRM, CM and DWBA, and using three volume fractions: truncated inferred volume fraction (ϕ_{tr}) for $\phi<40\%$, directly measured volume fraction, and inferred volume fraction from resistivity measurement including all measurements.

Three volume fractions used in deriving the sound speed contrast were: measured volume fraction ϕ, inferred volume fraction from formation factor $\hat{\phi}$, and inferred truncated volume fraction $\hat{\phi}$ with $\phi<40\%$; the three models were TPRM, CM, and DWBA, respectively. The errors introduced by using the volume fractions inferred from resistivity measurements were about 1.5% (Fig. 9). However, using truncated volume fractions inferred from resistivity measurements reduces the error by 50%. This is an encouraging result, since by using the resistivity method, we can avoid any direct handling of animals involvement in measuring and inferring sound speed in the zooplankton.

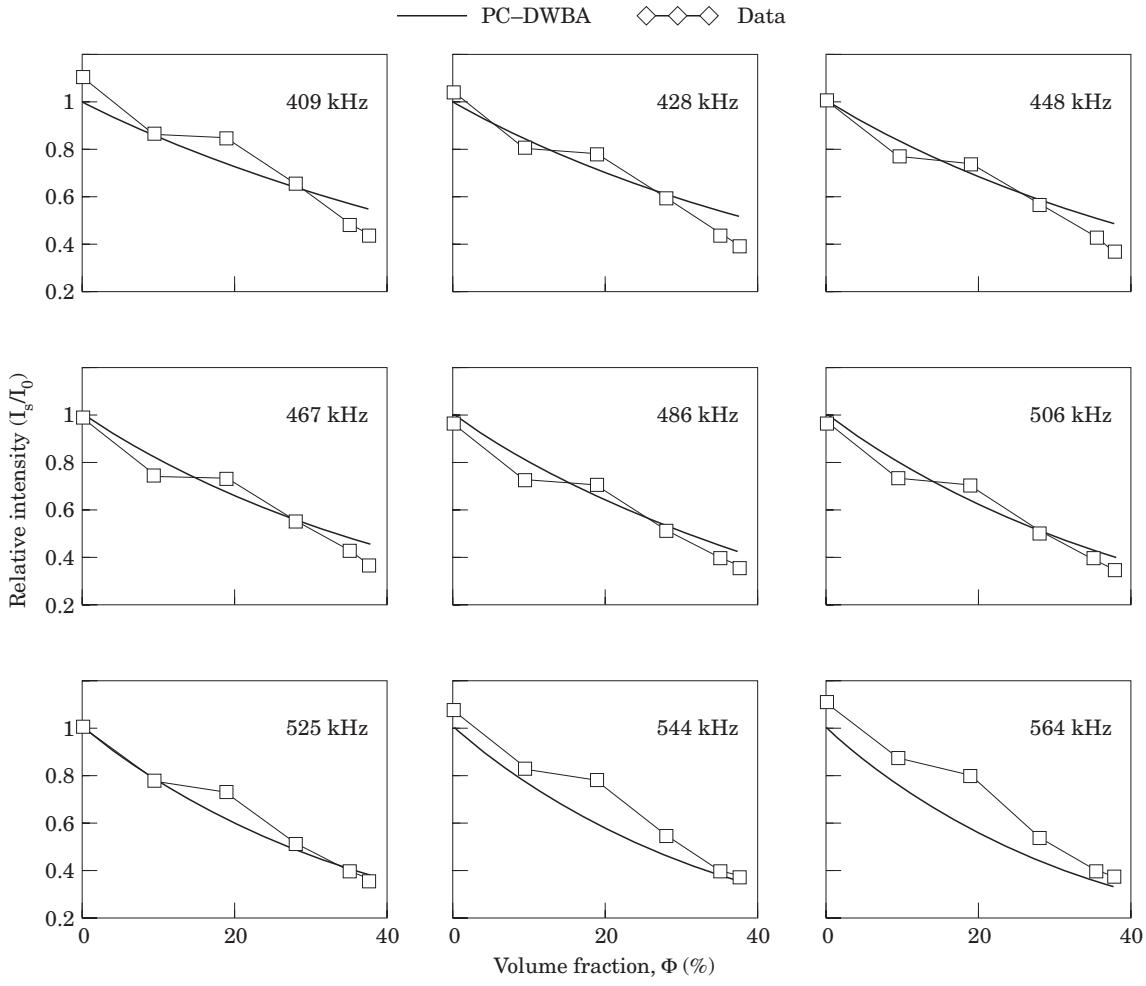

Figure 10. The comparison of theoretical predictions with the experimental data: transmission loss versus volume fraction at different frequencies. Prolate spheroid targets were used for modelling. For modelling parameters, sound speed contrast, h, was previously determined from travel time measurements. Semi-minor axis, a, aspect ratio, e, and density contrast, g, are determined by least-square-fit of the phase-compensated DWBA to the measured data (time series). â, ê, and ĝ inferred from the best fit are 2.8 mm, 3.5 and 1.019, respectively as compared with measured 2.76 mm, 3.27, and 1.043, respectively.

Having obtained estimates of the sound speed contrast h, the density contrast can be determined with the help of attenuation measurements. Applying Equations (21)–(25), the density and average size of the organisms can be determined. In our computations, a prolate spheroid scattering model was chosen to describe the elongated objects. To apply the model to the current problem, i.e., to estimate density contrast in the forward scattering configuration, a modification of the model given in Chu and Ye, 1999 was needed (Appendix A). The modified model took into account the effect of reflections from the wall of the acoustic chamber. In using Equation (25), the frequency range was from 409 kHz to 564 kHz (6 dB bandwidth), the semi-minor axis varied from 1 mm to 5 mm, the aspect ratio from 3 to 9, and the density contrast g from 1.01 to 1.1. The estimated â, ê and ĝ from the least-square fit were 2.80 mm, 3.50 and 1.019, respectively. Compared to the measured a = 2.76 mm, e = 3.27, and g = 1.043, the estimated errors were less than 1.5%, 7.1%, and 2.4%, respectively. In determining the size parameters and the density contrast, we did not use any floating parameters. The resultant estimated total volume of the animals was then:

$$V_{tot} = n\langle V_{ind}\rangle = n\left(\frac{4\pi}{3}\hat{a}^3 e\right) = 24\left(\frac{4\pi}{3}\right)(0.28^3)(3.5) \approx 7.72\ \text{cm}^3. \quad (27)$$

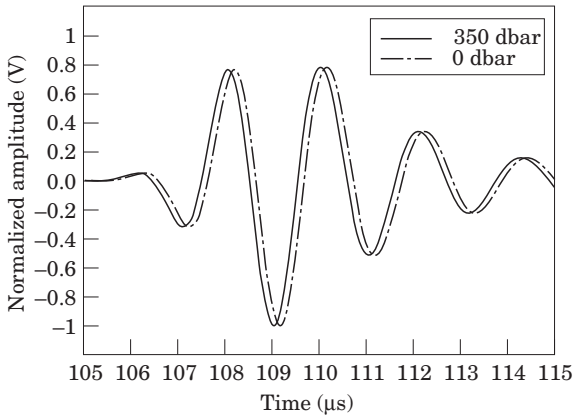

Figure 11. Received waveforms at different pressures. The increment of the sound speed in water due to pressure increment had been taken into account and removed. The resultant net increment of the sound speed contrast was about 2.0%.

Compared with the total measured volume, 6.0 cm^3, the estimate error was less than 30%. It is understandable that an underestimated density contrast has to be compensated by an overestimated scattering volume. In performing the non-linear optimization of Equation (25), further analysis indicates that the optimization is more sensitive to the size parameters than the density contrast. Systematic evaluation of the robustness of the optimization was not performed due to the limited amount of data sets. Since the model was only an approximate one and measuring errors were inevitable, the model-based inference of the density contrast may not be accurate. However, because of the fact that the forward scattering for weakly scattering scatterers is essentially proportional to the total volume of the scatterers, the forward scattering measurements are expected to be more stable than backscattering measurements. As a result, the inverted scattering parameters are believed to be reasonable. It should be pointed out that in this study, we only used PC-DWBA model because of its simplicity. Other models, such as deformed cylinder model (DCM) (Stanton, 1989; Ye *et al.*, 1997) may also be used in the optimization.

Comparisons of relative intensity versus volume fraction at different frequencies was made between model predictions and the data by incorporating the estimated parameters (Fig. 10). The agreement within the frequency band from 409 to 564 kHz was quite good. Although the estimated errors became larger outside this frequency band, the agreement could still be considered reasonable given the complexity of the problem.

The effect of pressure on the material properties of these shrimp was evident in two normalized waveforms at different pressures (Fig. 11). The waveform at 350 dbar was shifted towards the right to compensate for the sound speed increase of pure seawater due to pressure change. The relative change in sound speed contrast due to pressure can be shown to have a form of (Equation (B7), Appendix B):

$$\Delta h_{0-p} = \left(\Delta t_{m_{0-p}} - \frac{L-D}{L} \Delta t_{0-p} \right) \frac{c}{D\phi}, \tag{28}$$

where $(L - D/L) = \Delta t_{m_{0-p}} - L - D/L\Delta t_{0-p}$ is the effective time difference of sound propagating through the mixture at pressures of 0 dbar and 350 dbar. L and D are the total length of the acoustic chamber and the width of the animal compartment, respectively. ϕ is the volume fraction of the animals in the compartment. Inserting the measured parameters into Equation (28) and using the computed sound speed in water c with the measured salinity, 31.81 ppt and temperature, 5.4°C (Fofonoll and Millard, 1983), we have obtained $\Delta h_{0-p} = 0.02$. Although this is very small change, only about 2%, the resultant target strength deviation could be a few dB. However, if this same amount of Δh_{0-p} is for copepods, which are weaker scatterers, the target strength deviation could be as much as 20 dB, a factor of 100 in biomass estimate.

As for density contrast measurement under pressure, when applying pressure to the animals as described above, a slight volume reduction, 0.025 ml, was observed in a 10 ml mixture at pressure of about 350 dbar (500 psi). The net volume of the animals in the mixture was 3.85 ml. The volume reduction of pure seawater due to pressure was about 0.01 ml, or about 0.15% (Fofonoff and Millard, 1983). The net animal volume reduction was 0.015 ml, or about 0.4%. As in the sound speed case, although the variation was small, it could affect the target strength of a weaker scatterer significantly (Fig. 1).

Conclusions

Here the importance of the material properties to acoustic scattering by weakly scattering zooplankton (decapod shrimp) has been investigated. It is shown that since the sound speed and density contrasts of the zooplankton are very close to unity, a few percent change in h and g could result in as much as 20 dB deviation in target strength estimates.

A new laboratory device capable of inferring sound speed and density contrasts of zooplankton has been developed. It measures the travel time and the resistivity, as well as the scattering induced attenuation. The volume fraction of the animal can be obtained with resistivity measurement, which is necessary to infer sound speed contrast. It was found that if the volume fraction of the zooplankton was kept below 35%, the relative error of sound speed estimate caused by using inferred volume fraction was about 0.005. The inferred density

agreed with the measured density reasonably well; less than a 2.4% difference. This new device has a potential for *in situ* application to infer the material properties of the zooplankton.

Variability of the material properties due to changes in pressure was also investigated. It was found that the density contrast increases only slightly, about 0.4% with pressure increasing from zero to 350 dbar (500 psi), while sound speed contrast increased by as much as 2%, five times larger than the variation in density contrast.

Acknowledgements

The authors would like to thank K. Doherty and T. Hammer (Woods Hole Oceanographic Institution) for the mechanical design of the acoustic chamber and pressure vessel, T. Hammer for providing the mechanical schematic drawings, and Dr M. Jech (National Marine Fishery Service of NOAA, Woods Hole, MA) for his help in conducting the experiment. This work is sponsored by National Science Foundation, Grant No. OCE-9730680. This is Woods Hole contribution number 9988.

Appendix A

Since the model given by Equation (22) in Chu and Ye, 1999 was derived in a medium with no boundaries, to use the same formula for the current application in a wave guide, we need to take into account the reflections from the wall of the acoustic chamber. To simplify the problem, only the first order reflections are considered. This is reasonable, since multiple reflections can be removed in the time domain. Without reflections, the coefficient of Equation (22) of Chu and Ye, 1999 is:

$$h^2\gamma_k+\gamma_p\cos\theta_s=h^2\gamma_k+\cos\theta_s\gamma_p, \tag{A1}$$

where θ_s is the angle between the incident and receiving directions. The collective effects of the scattering from all animals, i.e. scattered from the animals first, reflected from the wall, and then to the receiver, are rather complicated to analyse rigorously, but an approximate method to estimate the mean effect may be used to reasonably account for this scattering-reflection effects. In Equation (A1), for forward scattering, the scattering angle, $\theta_{fs}=0$, while for scattered=reflected component, a mean scattering angle, θ_{sr}, may be used to represent the mean effect of the reflections. Hence a mean coefficient

$$\langle C_b\rangle=h^2\gamma_k+\gamma_p\cos\langle\theta_s\rangle, \tag{A2}$$

may be used to approximate the waveguide effects, where $\langle\theta_s\rangle$ is the effective mean scattering angle yet to be determined.

It is reasonable to use the scattered-reflected ray path from the centre of the animal compartment to the wall and then to the centre of the receiver as a "mean" path. The grazing angle associated with this path can be regarded as the mean scattering angle, $\langle\theta_{sf}\rangle$. From the parameters specified in Figure 3a, the angle is:

$$\langle\theta_{sf}\rangle=\operatorname{atan}\left(\frac{a_c}{z_c/2}\right)=\operatorname{atan}[1.27(\text{cm})/2.3(\text{cm})]=28.9^\circ, \tag{A3}$$

where $a_c=1.27$ cm (1/2″) is the radius of the animal compartment and $z_c=4.6$ cm is the distance between the centre of the animal compartment to the centre of the receiver ceramic (the potting material has a thickness of 1.0 cm from the ceramic to the front interface of the transducer). The material we used for the acoustic chamber is Delrin whose compressional sound speed and density are 2441.7 m/s and 1.41 g/cm^3, respectively. Using the measured sound speed in water 1468 m/s, the mean plane wave reflection coefficient is:

$$\langle R\rangle=\frac{\rho_D c_D\cos\langle\theta_{sr}\rangle-\rho c\cos\langle\theta_{st}\rangle}{\rho_D c_D\cos\langle\theta_{sr}\rangle-\rho c\cos\langle\theta_{st}\rangle}, \tag{A4}$$

where ρ_D and c_D are density of and sound speed in delrin, respectively. $\langle\theta_{sr}\rangle$ is the complement angle of the mean grazing angle $\langle\theta_{sf}\rangle$, i.e. $\langle\theta_{sr}\rangle=\pi/2-\langle\theta_{sf}\rangle$. $\theta_{st}=\operatorname{asin}(c/c_D\sin\theta_{sr})$ is the refracted angle. The resultant cosine of the mean scattering coefficient can be evaluated by taking the average of the forward scattering component ($\theta_{fs}=0$) and the scattered reflected component (associated with θ_{sf}):

$$\cos\langle\theta_s\rangle=\frac{\cos\theta_{fs}+|\langle R\rangle|\cos\langle\theta_{sf}\rangle}{1+|\langle R\rangle|}\approx 0.94, \tag{A5}$$

where we have used $\theta_{fs}=0$ and $|\langle R\rangle|=1$, indicating a total reflection, obtained from Equation (A4). Substituting $\cos\langle\theta_s\rangle$ into Equation (A2), we obtain the modified forward scattering coefficient. Since such a modification is small, it basically does not affect the sound speed estimation. It should be noted that the above approach is a crude approximation, since it not only uses a mean scattering angle to approximate the complicated problem involving the transmission through and the scattering by a cloud of scatterers in a waveguide, but also ignores the lateral wave and phase shift associated with the total reflections.

Appendix B

Referring to Figure 2b, we can write travel time equations for acoustic wave propagating through the animal-water mixture at two different pressures:

$$t_{m_0} = \frac{D}{c_{m_0}} + \frac{L-D}{c_0} \tag{B1}$$

$$t_{m_p} = \frac{D}{c_{m_p}} + \frac{L-D}{c_p} \tag{B2}$$

$$\Delta t_{m_{0-p}} = D\left(\frac{1}{c_{m_0}} - \frac{1}{c_{m_p}}\right) + (L-D)\left(\frac{1}{c_0} - \frac{1}{c_p}\right), \tag{B3}$$

where subscripts 0 and p stand for at pressure 0 and p, respectively. Since $t_0 = L/c_0$ and $t_p = L/c_p$ are travel times at pressure 0 and p without animal present, we obtain:

$$\Delta t_{m_{0-p}} = D\left(\frac{1}{c_{m_0}} - \frac{1}{c_{m_p}}\right) + \frac{L-D}{L}\Delta t_{0-p}, \tag{B4}$$

with

$$\Delta t_{0-p} = L\left(\frac{1}{c_0} - \frac{1}{c_p}\right). \tag{B5}$$

In addition,

$$\begin{aligned}\frac{1}{c_{m_0}} - \frac{1}{c_{m_p}} &= \frac{1}{c_0}\left[\frac{1}{h_{m_0}} - \frac{1}{h_{m_p}}\left(\frac{c_0}{c_p}\right)\right] \\ &\approx \frac{h_{mp} - h_{m_0}}{c_0 h_{m_p} h_{m_0}} \\ &\approx \frac{1}{c_0}\Delta h_{m_{0-p}} \\ &\approx \frac{1}{c_0}\phi\Delta h_{0-p},\end{aligned} \tag{B6}$$

where h_{m_0} being the sound speed contrast of the mixture to the surrounding seawater at pressure 0 dbar, while h_{m_p} being at pressure p. The last step comes from Equation (17). Substituting Equation (B6) into Equation (B4) and rearraging it, we obtain the final result:

$$\Delta h_{0-p} = \left(\Delta t_{m_{0-p}} - \frac{L-D}{L}\Delta t_{0-p}\right)\frac{c_0}{D\phi}, \tag{B7}$$

where we have ignored the change in volume concentration ϕ due to pressure. Note that $\Delta t_{m_{0-p}}$ and Δt_{0-p} in the equation are two directly measurable quantities. Since sound speed in water at atmosphere, c_0, the width of the animal compartment D, total length of the acoustic chamber L, and the animal volume concentration, ϕ are known, the change in sound speed contrast due to pressure change can be determined by Equation (B7).

References

Anderson, V. C. 1950. Scattering by a fluid sphere. J. Acoust. Soc. Am., 22: 426–431.

Archie, G. E. 1942. The electrical resistivity log as an aid in determining some reservoir characteristics. Trans. AIME, 146: 54–62.

Chu, D., Stanton, T. K., and Wiebe, P. H. 1992. Frequency dependence of sound backscattering from live individual zooplankton. ICES J. Mar. Sci., 49: 97–106.

Chu, D., Foote, K. G., and Stanton, T. K. 1993. Further analysis of target strength measurements of Antarctic krill at 38 kHz and 120 kHz: comparison with deformed cylinder model and inference of orientation distribution. J. Acoust. Soc. Am., 93: 2985–2988.

Chu, D., and Ye, Z. 1999. A phase-compensated DWBA representation of the bistatic scattering by weakly scattering objects: Application to zooplankton. J. Acoust. Soc. Am., 106: 1732–1743.

Evans, Rob. L. 1994. Constraints on the large-scale porosity and permeability structure of young oceanic crust from velocity and resistivity data. Geophys. J. Int., 119: 869–879.

Faran, J. J. 1951. Sound scattering by solid cylinders and spheres. J. Acoust. Soc. Am., 23: 405–418.

Fofonoff, P., and Millard, R. C. Jr 1983. Algorithms for computation of fundamental properties of seawater. Unesco Tech. Pap. in Mar. Sci., 44: 53.

Foote, K., Everson, I., Watkins, J. L., and Bone, D. 1990a. Target strength of Antarctic krill *Euphausia superba* at 38 and 120 kHz. J. Acoust. Soc. Am., 87: 16–24.

Foote, K. 1990b. Speed of sound in *Euphausia superba*. J. Acoust. Soc. Am., 87: 1405–1408.

Foote, K. G., Ona, E., and Toresen, R. 1992. Determinating the extinction cross section of aggregating fish. J. Acoust. Soc. Am., 91: 1983–1989.

Foote, K. G., Knutsen, T., Bekkevold, A. E., Dalpadado, P., and Johannessen, S. E. 1996. Initial, collateral measurements of some properties of calanus finmarchicus. ICES CM 1996/ L.21 Ref. B, pp. 2.

Frost, B. W., and McCrone, L. E. 1974. Vertical distribution of zooplankton and myctophid fish at Canadian weather station P, with description of a new multiple net trawl. Proc. Int. Conf. Engineering in the Ocean Environment, Halifax, Nova Scotia. IEEE J. Ocean. Eng., OE-1: 159–165.

Furusawa, M., Ishii, K., and Miyanohana, Y. 1992. Attenuation of sound by schooling fish. J. Acoust. Soc. Am., 92: 987–994.

GLOBEC 1991. GLOBEC Workshop on Acoustical Technology and the Integration of Acoustical and Optical Sampling Methods. Global Ocean Ecosystems Dynamics Report No. 4.

GLOBEC 1993. GLOBEC RPT. No. 3 on Sampling and Observation Systems. GLOBEC-International Chesapeake Biological Laboratory, pp. 16–22.

Greene, C. H., Wiebe, P. H., Burczynski, J., and Youngbluth, M. J. 1988. Acoustical detection of high density demersal krill layers in the Submarine Canyons off Georges Bank. Science, 241: 359–361.

Greene, C. H., Stanton, T. K., Wiebe, P. H., and McClatchie, S. 1991. Acoustic estimates of Antarctic krill. Nature, 349: 110(L).

Greene, C. H., Wiebe, P. H., and Zamon, Z. E. 1994. Acoustic visualization of patch dynamics in oceanic ecosystem. Oceanography, 7: 4–12.

Greenlaw, C. F. 1977. Backscattering spectra of preserved zooplankton. J. Acoust. Soc. Am., 62: 44–52.

Gross, F., and Raymont, J. E. G. 1942. The specific gravity of *Calanus finmarchicus*. Proc. Roy. Soc. Edinb. B., 61: 288–296.

Holliday, D. V., and Pieper, R. E. 1980. Volume scattering strengths and zooplankton distribution at acoustic frequencies between 0.3 and 3 MHz. J. Acoust. Soc. Am., 67: 135–146.

Holliday, D. V., Pieper, R. E., and Kleppel, G. S. 1989. Determination of zooplankton size and distribution with multi-frequency acoustic technology. Journal du Conseil International pour L'Exploration de la Mer, 46: 52–61.

Holliday, D. V., and Pieper, R. E. 1995. Bioacoustical oceanography at high frequencies. ICES J. Mar. Sci., 52: 279–296.

Ishimaru, A. 1978. Wave Propagation and Scattering in Random Media, Vol. I, ch. 1, pp. 14–15, Vol. II, ch. 14, pp. 265–268. Academic Press, New York.

Jackson, P. D., Smith, D. T., and Stanford, P. N. 1978. Resistivity-porosity-particle shape relation for marine sands. Geophy., 43: 1250–1268.

Kogeler, J. W., Falk-Petersen, S., Kristensen, A., Pettersen, F., and Dalen, J. 1987. Density- and sound speed contrasts in sub-Arctic zooplankton. Polar Biol., 7: 231–235.

Lax, M. 1951. Multiple scattering of waves. Rev. Mod. Phys., 25: 287–310.

Linderstrom-Lang, K. 1937. Dilatometric ultra-micro-estimation of peptidase activity. Nature, 139: 713–714.

Linderstrom-Lang, K., Jacobson, O., and Johnson, G. 1938. On the measurement of deuterium content in mixtures of H_2O and D_2O. C. R. Lab. Carlsberg (Sér. chim), 23: 17–26.

Lowndes, A. G. 1942. The displacement method of weighting living aquatic organism. J. Mar. Biol., 25: 555–574.

Miller, C. B., and Judkins, D. C. 1981. Design of pumping for sampling zooplankton with descriptions of two high capacity samples for coastal studies. Biol. Oceanogr., 1: 29–56.

Mualem, Y., and Friedman, S. P. 1991. Theoretical prediction of electrical conductivity in saturated and unsaturated soil. Water Resour. Res., 27: 2771–2777.

Salzen, E. A. 1956. The density of the eggs of *Calanus finmarchicus*. J. Mar. Biol. Ass. U.K., 35: 549–554.

Schopper, J. R. 1967. A theoretical investigation on the formation factor/permeability/porosity relationship using a network model. Geophys. Prospect., 14: 301–341.

Sheng, J., and Hay, A. E. 1988. An examination of the spherical scatter approximation in aqueous suspensions of sand. J. Acoust. Soc. Am., 83: 598–610.

Stanton, T. K., Nash, R. D. M., Eastwood, R. L., and Nero, R. W. 1987. A field examination of acoustical scattering from marine organisms at 70 kHz. IEEE J. Ocean. Eng., OE-12: 339–348.

Stanton, T. K. 1988. Sound scattering by cylinders of finite length I: Fluid cylinders. J. Acoust. Soc. Am., 83: 55–63.

Stanton, T. K. 1989. Sound scattering by cylinders of finite length III: deformed cylinders. J. Acoust. Soc. Am., 86: 691–705.

Stanton, T. K., Chu, D., Wiebe, P. H., and Clay, C. S. 1993. Average echoes from randomly oriented random-length finite cylinders: Zooplankton models. J. Acoust. Soc. Am., 94: 3463–3472.

Stanton, T. K., Wiebe, P. H., Chu, D., and Goodman, L. 1994a. Acoustic characterization and discrimination of marine zooplankton and turbulence. ICES J. Mar. Sci., 51: 469–479.

Stanton, T. K., Wiebe, P. H., Chu, D., Benfield, M. C., Scanlon, L., Martin, L., and Eastwood, R. L. 1994b. On acoustic estimates of zooplankton biomass. ICES J. Mar. Sci., 51: 505–512.

Stanton, T. K., Chu, D., and Wiebe, P. H. 1998a. Sound scattering by several zooplankton groups. I. Experimental determination of dominant scattering mechanisms. J. Acoust. Soc. Am., 103: 225–235.

Stanton, T. K., Chu, D., and Wiebe, P. H. 1998b. Sound scattering by several zooplankton groups. II. Scattering Models. J. Acoust. Soc. Am., 103: 236–253.

Telford, W. M., Geldart, L. P., Sheriff, R. E., and Keys, D. A. 1984. Applied Geophysics. Cambridge University Press, New York. Chapter 4.

Thorne, P. D., Vincent, C. E., Hardcastle, P. J., Rehman, S., and Pearson, N. 1991. Measuring suspended sediment concentrations using acoustic backscatter devices. Marine Geology, 98: 7–16.

Urick, R. J. 1947. A sound velocity method for determining the compressibility of finely divided substance. J. Appl. Phys., 18: 983–987.

Wiebe, P. H., Boyd, S., and Cox, J. L. 1975. Relationships between zooplankton displacement volume, wet weight, dry weight, and carbon. Fish. Bull., 73: 777–786.

Wiebe, P. H., Burt, K. H., Body, S. H., and Morton, A. W. 1976. A multiple opening/closing net and environmental sensing system for sampling zooplankton. J. Mar. Res., 34: 341–345.

Wiebe, P. H. 1988. Functional regression equations for zooplankton displacement volume, wet weight, dry weight, and carbon: A correction. Fish Bull., 86: 833–835.

Wiebe, P. H., Greene, C. H., Stanton, T. K., and Burczynski, J. 1990. Sound scattering by live zooplankton and micronekton: empirical studies with dual-beam acoustic system. J. Acoust. Soc. Am., 88: 2346–2360.

Wiebe, P. H., and Greene, C. H. 1994. The use of high frequency acoustics in the study of zooplankton spatial and temporal pattern. Proc. NIPP Symp. Polar Biol., 7: 133–157.

Wiebe, P. H., Mountain, D., Stanton, T. K., Greene, C. H., Lough, G., Kaartvedt, S., Manning, J., Dawson, J., Martin, L., and Copley, N. 1996. Acoustical study of the spatial distribution of plankton on Georges Bank and the relationship betwen volume backscattering strength and taxonomic composition of the plankton. Deep-Sea Research II, 43: 1971–2001.

Wiebe, P. H., Stanton, T. K., Benfield, M. C., Mountain, D. G., and Greene, C. H. 1997. High-frequency acoustic volume backscattering in the Georges Bank coastal region and its interpretation using scattering models. IEEE J. Ocean. Eng., OE-22: 445–464.

Winsauer, W. O., Shearin, H. M. Jr, Masson, P. H., and Williams, M. 1952. Resistivity of brine-saturated sands in relation to pore geometry. Bull. Amer. Assoc. Petrol. Geol., 36: 253–277.

Wyllie, M. R. J., Gregory, A. R., and Gardener, G. H. F. 1958. An experimental investigation of factors affecting elastic wave velocities in porous media. Geophysics, 23: 459–493.

Ye, Z. 1996. Theoretical description of possible detection of swimbladdered fish in forward scatter. J. Acoust. Soc. Am., 98: 2717–2725.

Ye, Z., Hoskinson, E., Dewey, R. K., Ding, L., and Farmer, D. M. 1997. A method for acoustic scattering by slender bodies. I. Theory and verification. J. Acoust. Soc. Am., 102: 1964–1976.

Ye, Z., and McClatchie, S. 1998. On inferring speed of sound in aquatic organisms. J. Acoust. Soc Am., 103: 1667–1670.

Yeh, C. 1967. Scattering of acoustic waves by a penetrable spheroid. I. Liquid prolate spheroid. J. Acoust. Sc. Am., 42: 518–521.